Analysis of Virus Transmission: A Stochastic Transition Model Representation of Epidemiological Models

C. Gourieroux *, J. Jasiak ‡

first version: March 31, 2020
revised: November 17, 2020

The growing literature on the transmission of COVID-19 relies on various dynamic SIR-type models (Susceptible-Infected-Recovered). For ease of comparison and specification testing, we introduce a common stochastic representation of the SIR-type epidemiological models. This representation is a discrete time transition model, which allows for classifying the epidemiological models with respect to the number of states (compartments) and their interpretation. Additionally, the (stochastic) transition model eliminates several limitations of the (deterministic) continuous time epidemiological models, which are pointed out in the paper. We show that when data on aggregate compartment counts are available, all discrete time SIR-type models admit a nonlinear (pseudo) state space representation and can be consistently estimated and updated from an extended Kalman filter.

Keywords: Covid-19, Epidemiological Model, SIR Model, Transition Model, State-Space Representation.

*University of Toronto, Toulouse School of Economics and CREST, *e-mail*: gouriero@ensae.fr
‡York University, Canada, *e-mail*:jasiakj@yorku.ca
The authors gratefully acknowledge financial support of the Chair ACPR: Regulation and Systemic Risks, the Agence Nationale de la Recherche (ANR-COVID) grant ANR-17-EUR-0010, and the Natural Sciences and Engineering Council of Canada (NSERC). We thank A. Monfort and an anonymous referee for helpful comments.

1 Introduction

For almost 100 years following the introductory article of Kermack, McKendrick [33], the SIR (Susceptible-Infected-Recovered) model has remained the primary tool of analysis for epidemiological studies and has inspired a considerable number of extensions [see e.g. [29], [9], [51] for an overview]. However, in recent applications to the Coronavirus pandemic, the results and forecasts obtained from SIR-type models may lack robustness. This concerns especially the conditions of collective (herd) immunity, and the size and timing of the peak of the epidemic. Moreover, the results can vary across the SIR-type models [see e.g. [14] for estimation in an early phase of the epidemic and [34] for a simulation study of the reproduction number R_0 estimator].

This paper introduces a common stochastic representation of SIR-type epidemiological models to facilitate the comparison between the models and their outcomes. This representation is a discrete time transition model, which is used to define a typology of epidemiological models with respect to the number of states (or compartments in the epidemiological terminology), their interpretation and the causal structure of time dependent transition matrices.

The discrete time transition model is characterized by a transition matrix, which determines the probabilities of transitions between the states (compartments) distinguished in an epidemiological model. As such, it can easily accommodate individual and aggregate count data sampled at various frequencies. In contrast, when a continuous time deterministic differential system is adapted to data sampled at a fixed interval, a discretization bias arises. This discretization bias affects the estimated collective (herd) immunity ratio and renders uncertain its reliability and even existence. Moreover, a time discretized SIR-type model is shown to provide different results in applications to data sampled at various frequencies, such as the daily or weekly frequencies, due to its lack of robustness with respect to the time unit. In particular, this concerns the reproduction number, which is a commonly used epidemiological parameter. As, in practice, the aggregate epidemiological data are updated daily, a one day timestep is adopted as the time unit of our discrete time stochastic transition models.

When the (cross-sectional) aggregate counts are observed, all SIR-type models are shown to have a (Gaussian) (pseudo) nonlinear state space representation, which is con-

venient for statistical inference. We demonstrate that a quasi-maximum likelihood (QML) estimation method can be applied to this pseudo state space representation by using numerical optimization with an extended, or unscented Kalman filter algorithm for approximating the unobserved state probabilities.

The paper is organized as follows. The stochastic transition model is introduced in Section 2. First, we define the stochastic framework of individual histories, which is next transformed into a deterministic dynamic model for the cross-sectional count aggregates over an infinitely large number of individuals. Section 3 examines the features of the 2-state SI and 3-state SIR models. We perform the sensitivity analysis to see how the peak of new infections and the time-to-peak depend on the transmission parameters. In Section 4, the (pseudo) state space representation of an epidemiological model is derived for statistical inference. In Section 5, we discuss the case when the transmission function displays either a deterministic, or stochastic variation over time. We show that these extensions of the model can also be examined in a (pseudo) state space framework. Section 6 concludes. The typology of SIR type models with more than 2 states is given in Appendix 1. Proofs are gathered in Appendix 2.

2 Contagion Modelling

This Section introduces a general specification that encompasses the main epidemiological SIR-type models. It is a discrete time stochastic transition model that allows for modelling of individual histories during an epidemic while avoiding the limitations of a time discretized continuous time deterministic epidemiological model, such as the following: The time discretized version of a continuous time SIR-type model may depend on the time unit and need to be re-adjusted for the sampling frequency of the data. Moreover, the reproduction number computed from the time discretized model depends on the time unit as well, and takes a different value when computed from daily or weekly data. As mentioned earlier in the Introduction, we consider the daily frequency.

2.1 The Stochastic Transition Model

We consider a large panel of individual histories $Y_{i,t}, i = 1, .., N, t = 0, .., T$, where the variable Y is qualitative polytomous with J alternatives denoted by $j = 1, ..., J$. These

alternatives are the states of infection, recovery, or death, depending on the model specification. The discrete time t is assumed to be measured in days, as daily data are commonly used in epidemiological studies.

Assumption A1: The individual histories are such that:

i) The variables $Y_{i,t}, i = 1, .., N$ at time t fixed have the same marginal (i.e. cross-sectional) distribution. This common distribution depends on time t and is discrete. It is determined by the vector $p(t)$ of size J with components:

$$p_j(t) = P(Y_{i,t} = j),\ j = 1, .., J.$$

These components are non-negative and sum up to 1 .

ii) The processes $(Y_{i,t}, t = 1, ., T), i = 1, .., N$, are independent, heterogeneous Markov processes of order 1, with common transition probabilities. The transitions from date $t-1$ to date t are characterized by the $J \times J$ transition matrix $\Pi[p(t-1)]$. This matrix has nonnegative elements and each of its rows sums up to 1.

The vector $p(t)$ represents the cross-sectional (marginal) probabilities of states. In practice, the cross-sectional probability $p(t)$ is close to the cross-sectional frequency $f(t)$, computed from the values of $Y_{i,t}$. Then, transition matrix $\Pi[p(t-1)]$ is close to $\Pi[f(t-1)]$. However the transitions between states have to be defined with respect to $p(t-1)$ to remain independent of the population size.

Assumption A2: i) The epidemic starts at time 0. ii) At time 0 all individuals are in state $j = 1$, which is interpreted as the susceptible compartment.

Under Assumptions A1 and A2, the individual histories $Y_{i,t}$ are independent and identically distributed. Therefore, the individuals are exchangeable, i.e. have similar risk factors (homogenous population).

The initial condition implies nonstationary evolutions of the processes of individual histories over time. This nonstationarity and the time dependence of the transition matrix through $p(t-1)$ only are the distinct characteristics of a SIR-type model. There is one exception, however: When the SIR model is a homogenous Markov process, the transition matrix Π is independent of $p(t-1)$.

In general, the transition matrix Π is time dependent. Then, the structural epidemiological model is determined by the number of states, their interpretations, and the causal

structure of the transition matrix. More specifically, the elements of the transition matrix can be either zeros, constants, or functions of marginal probabilities $p(t-1)$, which is a special form of time dependence. The models differ with respect to the form of those functions and of the components of $p(t-1)$, which are their arguments.

The examples of commonly used SIR-type specifications are described in Appendix 1. Although most of the SIR-type models are heterogeneous Markov models, the homogeneous Markov model mentioned above can be used for either a local analysis (see Section 2.2), or for deriving the lower and upper bounds on the trajectories of marginal probabilities $p(t)$. Those bounds are mainly determined by the maximum (resp. minimum) of moduli of all eigenvalues of $\Pi[p(t-1)]$ over time t, called the Lyapunov exponents.

2.2 The Deterministic Model

Assumptions A1 and A2 defining the stochastic dynamics of $Y_{i,t}$ lead to a deterministic nonlinear recursive model for the dynamics of marginal probabilities $p(t)$. This deterministic representation (or mechanistic model, see [10]) is obtained by applying the Bayes formula and is given by:

$$p(t) = \Pi\left[p(t-1)\right]' p(t-1),\ t = 1, .., T, \tag{2.1}$$

with initial condition: $p(0) = (1, 0, .., 0)'$. As shown in Section 4, system 2.1 can be used as a system of estimating equations for statistical inference, if the frequency counterparts of $p(t)$ are observed.

System 2.1 can be rewritten to define the dynamics of changes in marginal probabilities:

$$\Delta p(t) = p(t) - p(t-1) = \{\Pi\left[p(t-1)\right] - Id\} p(t-1), \tag{2.2}$$

where Id denotes the identity matrix. The equation 2.2 highlights the role of the generator: $\Pi\left[p(t-1)\right] - Id$, in determining the changes in marginal probabilities $\Delta p(t)$.

Remark 1: Discretization bias.

A major part of literature considers epidemiological models written as deterministic differential systems in continuous time. A continuous time analogue of the deterministic model 2.2 is:

$$dp(t)/dt = \{\Pi[p(t)] - Id\}p(t). \tag{2.3}$$

In general, the system of equations 2.2 is not the exact time discretized version of the continuous time system 2.3 [see Appendix 2 for the example of a rational recursive system in the SI model]. Thus, due to the nonlinearities in the dynamics, a chaos effect can arise and induce considerably different evolutions of $p(t)$ defined from 2.2 and 2.3, especially over the medium and long run.

To highlight the differences between the discrete and continuous time modelling, let us consider the 2-state SIS model with a linear force of infection, i.e. a linear function π (see Appendix 1). The probability of being infected $p_2(t)$ satisfies the following recursive equation [1]:

$$p_2(t) = [\beta p_2(t-1)][1 - p_2(t-1)] + (1-\gamma)p_2(t-1),$$

in discrete time and

$$dp_2(t)/dt = bp_2(t)[1 - p_2(t)] - cp_2(t),$$

in continuous time. Even though both equations look similar and contain similar parameter symbols, the following differences can be pointed out:

i) The discrete time version of the SIS model is not time consistent, as $p_2(t)$ at lag 2 derived by recursive substitution is a quartic function of $p_2(t-2)$. Hence, this specification needs to be modified whenever the timestep between observations changes. In practice, this means that a specification valid for daily data is not valid for weekly data. On the contrary, the continuous time version of SIS model is time consistent.

ii) The parameters (β, γ) and (b, c) in both the discrete and continuous time SIS models given above depend on the selected time unit too. In the continuous time model however, the contagion parameters b and the recovery intensity c are multiplied by the same factor when the time unit is changed. Then, the reproduction number R_0 defined as the

[1] Coefficients β, γ are assumed constrained to ensure that $p_2(t)$ takes values between 0 and 1, for any $p_2(t-1)$ in [0,1].

expected number of individuals infected by a new infected individual during his/her infectious episode is equal to $R_0 = b/c$ [2]. It is also invariant with respect to the time unit. As the discrete time model is not time consistent, the reproduction number computed directly from the time discretized model $R_0^* = \beta/\gamma$ is not invariant with respect to the time unit either. Hence, different values of R_0^* are obtained from daily and weekly data. Any result obtained from the time discretized differential equation (called the Euler discretization) and interpreted in the continuous time framework needs to be used with caution. This finding calls into question the reliability of the estimated reproduction number R_0 and some of its transforms, such as the asymptotic value $p_2(\infty)$, which are important components of epidemiological studies.

iii) Although it is common to approximate the trajectory of a continuous time model by a trajectory of one of its Euler discretizations with a small time unit [see e.g. [17], Section 3.1], these two trajectories can still be quite different even if the timestep is small. This difficulty has been first revealed in the SIR model with linear contagion, for which the exact solution in continuous time has been derived [27]. More precisely, let us consider a SIR model with a transmission function $\pi_{11}(p) = a(p_1)p_2$ that depends also on the proportion of susceptibles (i.e. the population-at-risk). For some specifications of function $a(.)$, the continuous time model has no collective immunity. Yet, the trajectories of crude Euler discretizations of this SIR model always show the collective immunity exists [see, [3], [10], Section 2.1]. In some sense, the notion of collective immunity is entirely model-based, and is not robust with respect to changes from discrete to continuous time.

Remark 2: Non-differentiability of a continuous time frequency model

It is common to write the epidemiological model as a differential system of frequencies $f(t)$ computed by dividing the counts in each compartment by the population size, instead of marginal probabilities $p(t)$, as follows:

$$df(t)/dt = [\Pi[f(t)] - Id]f(t), \tag{2.4}$$

[see e.g. [17], eq. (2.1) and eq. (2.2)]. This differential system is not compatible with the set of admissible values of vectors $f(t)$ [3]. The components of $f(t)$ are not continuously

[2] R_0 has the same expression in the SIR and SI models, as the SI model is the special case of the SIR model (see, Section 3.2.1).

[3] It is also the case when a stochastic feature is introduced by replacing the deterministic differential

valued functions, as they take on values equal to the multiples of $1/N$, which implies the non-differentiability of function $f(t)$. Therefore, this type of representation is misleading. Moreover, as the model is deterministic, it cannot take into account the ex-ante uncertainty about vectors $f(t)$, which are random.

2.3 Local Expansions

Let us now examine the dynamics of marginal probabilities of states $p(t)$. The analysis of their evolution during an epidemic can be simplified if we focus on either the beginning, or the end of the epidemic and consider local expansions.

2.3.1 Beginning of the epidemic

At time $t = 0$, the initial value is: $p(0) = (1, 0, .., 0)'$. Below, we consider expansions of orders 1 and 2 of the recursive system 2.1 in a neighbourhood of $p(0)$.

i) First-order expansion:

The first-order expansion is:

$$p(t) = \Pi[p(0)]' p(t-1), \tag{2.5}$$

which corresponds to a homogeneous Markov model with transition matrix $\Pi[p(0)]$. It can be solved analytically as:

$$p(t) = \Pi\left[p(0)\right]'^{t} p(0), \tag{2.6}$$

We find that locally the components of marginal probabilities $p(t)$ are combinations of exponential functions (and also of sine functions, cosine functions, which can possibly be multiplied by polynomials, if some eigenvalues of $\Pi\left[p(0)\right]$ are complex and/or multiple). Their dynamics are constrained by the specific form of matrix $\Pi[p(0)]$, which is a transition matrix. More specifically, all components of $p(t)$ have to take values between 0 and 1. In order to satisfy this restriction, locally, the marginal probability $p_1(t)$ is exponentially decreasing over time, whereas marginal probabilities of other states $p_j(t),\ j = 2, .., J$ are exponentially increasing over time.

equation by a stochastic one, such as a multivariate Jacobi process to account for the positivity and unit mass restrictions on the components of $f(t)$ [see, [1], [31], [36] for examples of stochastic differential epidemic models and [21] for the multivariate Jacobi process].

ii) Second-order expansion

The second-order expansion leads to the dynamic system:

$$p(t) = \{\Pi\left[p(0)\right] + \sum_{j=1}^{J} d\Pi\left[p(0)\right]/dp_j \, p_j(t-1)\}' p(t-1), \tag{2.7}$$

which is a Riccati quadratic recursive system without a closed-form solution.

2.3.2 End of the epidemic

In general, the epidemiological models include some absorbing states, such as the states of deceased, or recovered (see, examples in Section 3 and Appendix 1). In this case, the sequence of marginal probabilities $p(t)$ has a limit when $t \to \infty : p(\infty)$, say. If there is only one absorbing state J, say, we can get $p(\infty) = (0, 0, .., 1)'$. Then, the first- and second-order expansions can be performed in a neighbourhood of $p(\infty)$, yielding dynamic approximations systems analogous to systems 2.5 and 2.7.

3 Examples

Let us now study the dynamic properties of two commonly used epidemiological models, which are the discrete time SI and SIR transition models, respectively (see Appendix 1). We derive the dynamic equations of marginal probabilities and describe their behavior at the beginning and the end of an epidemic.

3.1 SI Model

3.1.1 The deterministic model

The transition model representation of the deterministic SI model involves the following 2×2 transition matrix:

row 1, S: $1 - \pi(p_2)$; $\pi(p_2)$.

row 2, I: 0, 1.

The state I of infected, still infectious and immunized is the absorbing state. Function π is the contagion function (called the force of infection, or transmission function) that satisfies the following assumption:

Assumption A3: π is a non-decreasing function of p_2, which takes values between 0 and 1.

The value $\pi(0)$ can be interpreted as an exogenous component of the contagion. In an open economy, it can be due to the effect of tourism, international trade and migration. In a closed economy, such as the world in its entirety, it can be set equal to zero. There is a strict (endogeneous) contagion effect if function π is strictly increasing.

Example 1: A common specification of the force of infection π is the linear function: $\pi(p_2) = b\,p_2$, where parameter b takes values between 0 and 1, or a logistic function of p_2:

$$\pi(p_2) = \exp(a + bp_2)/[1 + exp(a + bp_2)],$$

where coefficient b is non-negative. In the logistic force of infection, the exogenous infection rate is measured by: $\exp a/[1 + \exp a]$ and the strict endogenous contagion effect by parameter b. Other functional forms have also been considered in the growth literature and obtained, for instance, by replacing p_2 by a power of p_2 in the expressions given above [see e.g. [44], [39], Table 1, [8], [54], [28]].

The form of the transition matrix given above leads to the following nonlinear recursive equation of order 1 for the marginal probability of being infected:

$$p_2(t) = \pi(p_2(t-1))[1 - p_2(t-1)] + p_2(t-1). \tag{3.1}$$

Proposition 1: Under Assumption A3, $p_2(t)$ is a non-decreasing function of time with exponential lower and upper bounds:

$1 - [1 - \pi(0)]^t \leq p_2(t) \leq 1 - [1 - \pi(1)]^t$.

It tends to 1 when $t \to \infty$. Hence, there is no collective immunity in the discrete time SI model.

Proof:

i) It is non-decreasing, as $p_2(t) - p_2(t-1)$ is non-negative.

ii) The bounds are obtained by observing that $p_2(t)$ is an increasing function of π.

iii) Since $p_2(t)$ is non-decreasing and bounded by 1, it converges to a value $p_2(\infty)$. This limit is equal to 1, by considering equation 3.1 at $t = \infty$.

QED

In particular, if there is no contagion effect, i.e. if $\pi(p_2)$ is constant and equal to π, then the marginal probability of being infected is: $p_2(t) = 1 - [1 - \pi]^t$.

3.1.2 Local Expansions

It is interesting to consider the expansions of the dynamics of the probability of being infected in the SI model at the beginning of the contagion,i.e. when p_2 is close to zero, or at the end of the contagion, i.e. when p_2 is close to 1.

i) Beginning of the contagion

A second-order expansion leads to:

$$p_2(t) - p_2(t-1) \propto [\pi(0) + d\pi(0)/dp\, p_2(t-1)][1 - p_2(t-1)]. \tag{3.2}$$

ii) End of the contagion

The second-order expansion in a neighbourhood of $p_2 = 1$ yields:

$$p_2(t) - 1 = [\pi(1) + d\pi(1)/dp\, [p_2(t-1) - 1]][1 - p_2(t-1)] + p_2(t-1) - 1. \tag{3.3}$$

Both approximations lead to discrete time logistic recursive equations for the probability of being infected $p_2(t)$ and the probability of not being infected $1 - p_2(t)$, respectively, although with different parameters.

3.1.3 Continuous time analogue

The continuous time analogue of the recursive equation 3.2 is:

$$dp_2(t)/dt = (\alpha + \beta p_2(t))(1 - p_2(t)), \tag{3.4}$$

where $\alpha = \pi(0), \beta = d\pi(0)/dp$ are both nonnegative.
Equation 3.4 can be solved analytically.

Proposition 2: i) Assuming that the beginning of the epidemics is at time $t = 0$, the solution of equation 3.4 is:

$$p_2(t) = [\alpha \exp[(\alpha + \beta)t] - \alpha]/[\alpha \exp[(\alpha + \beta)t] + \beta].$$

ii) If $\beta > \alpha$, the solution is such that the derivative $dp_2(t)/dt$ attains the maximum when $p_2(t) = (\beta - \alpha)/(2\beta)$. The time-to- inflection is reached at $t^* = \log(\beta/\alpha)/(\alpha + \beta)$.

Proof: see Appendix 2.

It follows that the probability of being infected $p_2(t)$ is a logistic function of time. Moreover, if the strict contagion effect is large as compared to the exogenous component of the contagion, there is a peak in the changes of ratios of infected individuals over time. The size and timing of the peak depend on the transmission parameters. However, the SI model has only two parameters, which is insufficient to independently determine the size of the peak, the time to peak and other characteristics such as the flatness of the curve at the peak (the so-called "plateau" effect) as well as the asymmetry of the curve with respect to the peak.

The above outcomes of the SI model 3.2 are based on a local expansion of the initial nonlinear recursive equation and are therefore valid at the beginning of an epidemic only. The length of the period of time over which such an expansion is valid depends on function π, and also on the values of parameters a, b in the parametric SI model in Example 1. There is no collective immunity in either continuous, or discrete time SI model.

3.1.4 Sensitivity analysis

Let us consider below the parametric SI model in Example 1 and illustrate graphically its dynamics. At time 0, we fix the probability of being infected $p_2(0) = 0$ and set the parameters α, β, where $\alpha > 0, \beta > 0$ equal to $\alpha = 0.005, \beta = 0.85$.

Figure 1 below displays the dynamic of solution $p(t)$ which satisfies the continuous time SI model 3.4, i.e. with the logistic evolution given in Proposition 2, and its discrete time Euler approximation at the beginning of an epidemic given in equation 3.2. It is computed with the same values of parameters α, β given above and the same time unit of one day. Figure 1 shows that the daily discrete time approximation 3.2 can be very misleading when it is used for forecasting over a medium, or long run.

[Insert Figure 1: Evolutions of $p(t)$, SI Model]

When $\beta < \alpha$, we get an increasing concave curve that tends to 1. When $\beta > \alpha$, as in Figure 1, we get an exponential convex increase for small t, followed by an increasing concave pattern of convergence to 1.

The evolutions of changes of $p(t)$ are shown in Figure 2:

[Insert Figure 2: Evolutions of Changes in p(t), SI Model]

When $\beta > \alpha$, we get a hump-shaped pattern with the curve decreasing at a slower rate

after the peak than increasing before the peak.
We complete the sensitivity analysis of the main features of the SI model by examining the size of peak (Figure 3) and the time-to-inflection (Figure 4) as functions of parameters α, β.

[Insert Figure 3: Size of Peak, SI Model]

[Insert Figure 4: Time-to-Inflection, SI Model]

3.2 SIR Model

3.2.1 The model

Let us now consider the SIR model (see Appendix 1) with three states: S for Susceptible; I for Infected, infectious, not immunized; R for Recovered, immunized and no longer infectious. Its transition model representation involves the 3×3 transition matrix, which is triangular and given by:

row 1, S: $1 - \pi(p_2)$; $\pi(p_2)$; 0
row 2, I : 0; p_{22}; p_{23}
row3,R : 0; 0; 1

where p_{23} is strictly positive, and R is the absorbing state.

In the limiting case $p_{23} = 0$, the 2×2 North-West subset of the transition matrix corresponds to the SI model discussed in Section 3.1, with two absorbing states in the SIR model: I and R. In this limiting case, state R cannot be reached starting from an initial state S of susceptible individuals.

The marginal probabilities of states I and R satisfy two linearly independent estimating equations:

$$\begin{aligned} p_2(t) &= \pi[p_2(t-1)][1 - p_2(t-1) - p_3(t-1)] + p_{22}p_2(t-1), \\ p_3(t) &= p_{23}p_2(t-1) + p_3(t-1). \end{aligned} \tag{3.5}$$

From the second equation of system 3.5,we get:

$$p_2(t-1) = [p_3(t) - p_3(t-1)]/p_{23}, \tag{3.6}$$

and, by substituting into the first equation, we derive the recursive equation satisfied by $p_3(t)$:

$$\begin{aligned} p_3(t) &= p_3(t-1) + \pi[(p_3(t-1) - p_3(t-2))/p_{23}][p_{23} - p_3(t-1) + (1-p_{23})p_3(t-2)] \\ &+ p_{22}[p_3(t-1) - p_3(t-2)]. \end{aligned} \tag{3.7}$$

Proposition 3 i) The sequence $p_1(t)$ [resp. $p_3(t)$] is decreasing [resp. increasing].

ii) The sequence $p_3(t)$ satisfies a nonlinear recursive equation of order 2.

iii) The sequence $p_2(t)$ is a linear moving average of order 1 in $p_3(t+1)$.

The higher order of temporal dependence in $p_3(t)$ is due to the interpretation of state I as a transitory state between states S and R. Thus, the dynamics of $p_3(t)$ has to account for both the entries into and exits from the state I.

Let us now discuss the behaviour of marginal probabilities p(t) when t tends to infinity. Since $p_3(t)$ is increasing, and is upper bounded by 1, its limit exists. It is denoted by $p_3(\infty)$. From equation 3.6, it follows that the limit of $p_2(t)$ is zero. Then, by taking into account the first equation of 3.5, we get:

Lemma 1: When $t \to \infty$,

i) $p_2(t)$ tends to 0.

ii) If $\pi(0)$ is different from 0, $p_3(t)$ tends to 1.

iii) If $\pi(0) = 0, p_3(t)$ might tend to a limiting value $p_3(\infty) < 1$.

Determining the conditions for a convergence to $p_3(\infty)$, strictly less than 1 and computing this limiting value, which is interpreted as the collective immunity ratio are common topics in the epidemiological literature. For the discrete time SIR model, it has been proven in [3] that $p_3(\infty)$ is always strictly less than 1. However, estimation errors on a long run parameter $p_3(\infty)$ are large in an early phase of epidemic. Hence, the estimated ratio of collective immunity may be unreliable.

3.2.2 Homogeneous Markov

As mentioned in Section 3.1, it is interesting to consider the homogeneous Markov chain, obtained when function π is constant (no contagion). Then, the evolution of $p(t)$ is

driven by a linear recursive equation of order 1: $p(t) = \Pi' p(t-1)$, where Π is a triangular matrix with eigenvalues: $1-\pi, p_{22}, 1$. The following proposition is obtained:

Proposition 4: For a constant π, we have: $p(t) = A(1-\pi)^t + Bp_{22}^t + C$, where A, B, C are 3-dimensional vectors.

The effects of entries into and exits from state I induce the two driving exponential functions.

When function π is not constant, the decreasing sequence $p_1(t)$ and increasing sequence $p_3(t)$ take values between their analogues computed from a homogeneous Markov chain with $\pi = \pi(0)$ and $\pi = \pi(1)$, respectively.

3.2.3 Sensitivity analysis

Let us assume a linear function $\pi(p_2) = a + bp_2$, where $a > 0, b > 0, a + b < 1$. Then the SIR model involves 3 independent parameters, and is expected to provide more flexibility than the SI model, due to the additional parameter p_{23}. Below, we perform a sensitivity analysis similar to the one in Section 3.1.4 and focused on series $p_2(t)$. Parameters a, b, p_{23} are set equal to $a = 0.005, b = 0.85, p_{23} = 0.5$.

[Insert Figure 5: Evolution of $p_2(t)$, SIR Model]

[Insert Figure 6: Evolution of Change in $p_2(t)$, SIR Model]

The timing of a peak is determined by parameter a as shown below. We hold parameter $b = 0.85$ constant and change the values of parameter a in Figure 7.

[Insert Figure 7: Timing of Peak, a varying, SIR Model]

Next, parameter $a = 0.005$ is held constant and the values of parameter b are allowed to vary. The size of peak is determined by parameter b as shown in Figure 8 below.

[Insert Figure 8: Size of Peak, b varying, SIR model]

4 Statistical Inference

This section presents the methods of inference for the discrete time transition models. We assume that the observational and model timesteps are equal.

If the individual histories, or a set of sufficient statistics for individual data were available, then the maximum likelihood (ML), or indirect inference estimators could be used.

For example, in the limiting case of a homogeneous Markov Chain, the ML estimator of the transition matrix is the matrix of transition frequencies that define a set of sufficient statistics [see e.g. [10] for estimation of compartmental model from flow data]. However, individual epidemiological data are rarely available and only aggregate counts are provided, such as the counts of new infections, and/or cross-sectional frequencies. Below, we discuss the case when the $f(t)$'s are observed [4]. This aggregation step makes difficult the derivation of the likelihood function of $f(t)$, which is commonly replaced by a misspecified likelihood function, i.e. a quasi-likelihood function. When the quasi-likelihood function is well chosen, the quasi-maximum likelihood estimators are consistent when the population size is large and time T is fixed, although not fully efficient. This is the setup examined below.

Let us now consider a parametric transition matrix $\Pi[p(t-1);\theta]$, with parameter vector θ, and assume that the empirical frequencies $f(t), t = 1, .., T$ are observed. In addition, we assume that this discrete time parametric model is well specified.

4.1 Distribution of Frequencies

Under Assumptions A1, A2, the observed frequencies $Nf(t)$ follow the multinomial distribution $M(N; p(t))$, at any time t, but have a rather complicated joint distribution. However, if the size of the population is large and the observed counts $Nf(t)$ not too small (i.e. larger than 10-20), these frequencies converge at rate $1/\sqrt{N}$ to their theoretical counterparts and are asymptotically normal. Thus we can write:

$$f(t) = p(t) + u(t), \tag{4.1}$$

where the errors $u(t)$ are Gaussian with mean zero and the variance-covariance matrix at lag h given below [22]:

$$Cov[u(t), u(t-h)] = (1/N)\{\Pi(t-1,h)diag[p(t-h)] - p(t)p(t-h)'\}, \tag{4.2}$$

where: $\Pi(t-1,h) = \Pi[p(t-1)]...\Pi[p(t-h)]$.

[4] For the SIR model, these frequencies are sufficient statistics. In general, there is a loss of information when the cross-sectional counts only are used.

This is a rather complicated serial dependence, which is due to the data aggregation. In particular, the series $f(t)$ is not Markov of finite order, as it is commonly assumed in state space models.

Remark 4: Regularity Condition

The regularity conditions for consistency and asymptotic normality are not satisfied at the very beginning of the epidemic, when for example the number of recoveries after initial infections is low. The regularity conditions are not satisfied either if too many compartments are introduced, for example, when taking into account the different stages of medical care. Then, multivariate Poisson approximations have to be used instead of normal approximations, which is out of the scope of this paper.

4.2 (Pseudo) State Space Representation

System 4.1 resembles a measurement equation in a state space system with the measurement variable $f(t)$, measurement error $u(t)$, and the following system of transition equations for the state variable $p(t)$,:

$$p(t) = \Pi[p(t-1); \theta]' p(t-1). \tag{4.3}$$

However, the system of equations 4.3 and 4.1 does not fully satisfy the definition of a state space representation because the measurement errors $u(t)$ are serially correlated, as shown in equation 4.2.

This difficulty is easily circumvented by assuming a pseudo Gaussian distribution for errors $u(t)$, and disregarding the serial correlation. Their variance-covariance matrix at time t can be assumed equal to an identity matrix Id (Ordinary Least Squares approach), or an unknown constant matrix Ω (Weighted Least Squares approach), or even the true expression of $V(u(t))$ can be considered. The latter one is strongly recommended, as it introduces appropriate weights during the outbreak and increases the efficiency of the QML estimator. Upon this change of autocovariance structure, a (pseudo) state space representation is obtained.

The parameters of the pseudo state space representation can be estimated by the Gaussian quasi-maximum likelihood (QML). The quasi-maximum likelihood approach has also an interpretation in terms of estimating equations and asymptotic least squares

[see, [6], [20], [40], [32], [26], [42]]. As the asymptotic theory is established for T fixed and $N \to \infty$, the QML methods provide consistent estimators of parameter vector θ, which are not fully efficient as the true structure of autocovariances of errors $u(t)$ has not been taken into account [see, [22], Appendix 2].

In practice, the QML estimates [5] of θ can be computed numerically from an extended, or unscented Kalman Filter [6] applied to the (pseudo) state space model. These versions of the Kalman filter are numerical algorithms for computing the QML estimates. They also provide standard errors, which need to be interpreted with caution, as they are not computed from the "sandwich" formula that correctly accounts for serial correlation.

The estimation approach outlined above remains valid when some frequencies $f_j(t)$ are missing (see [22], [11] for inference on latent counts of COVID-19 infected and undetected (asymptomatic) individuals).

The extended Kalman filter provides information on the uncertainty of estimates and predictions. This uncertainty has to be taken into account, especially at the early ascending phase of an epidemic, when the number of observations is small, the quality of data is rather poor and the parameter of interest, such as the peak, is distant in time from the period of observations. Then, the confidence and prediction intervals are rather wide and the statistician has to interpret the results with caution [see e.g. [50], [14] for studies at early stages].

The extended Kalman filter is suitable as an updating algorithm of estimates and forecasts [43]. This is especially important at the beginning of the epidemic, when each newly arrived observation is very informative.

5 Models with Time Dependent (Stochastic) Parameters

In Sections 3 and 4, we considered a deterministic transmission model and its estimation by a (pseudo) Kalman filter to account for the measurement errors. The approach can be extended to some stochastic transmission models while preserving a nonlinear (pseudo)

[5] As the QML approach does not account for the structure of the variance-covariance matrix of the $u(t)$'s it can be improved by replacing a "moment" estimator by a GMM estimator.

[6] see, e.g. [47], [37] for the Extended Kalman Filter.

state space representation. The aim is to distinguish the intrinsic uncertainty due to the stochastic transmission from the observational uncertainty due to a large, but finite size of the population at risk. Three types of stochastic epidemiological models have been introduced in the literature:

i) Continuous time models in which the differential system is replaced by a stochastic differential system by adding Brownian motions to the equations. This extension has no clear structural interpretation [see e.g. [31], [17], [45], [55], [36]] [7].

ii) Discrete time models with a stochastic duration of the incubation period. In a model with a linear transmission function, this is commonly done by assuming a gamma or Erlang duration distribution [see e.g. [5], [38], [34], Section 5.b, [13]]. This leads back to a model with deterministic transmission and an increased number of compartments corresponding to different possible (discrete) duration values, when the stochastic duration is integrated out.

iii) It is also possible to transform the transmission function into a stochastic transmission function. When the transmission function is linear $\pi(p_t) = ap_t$, the intensity parameter can be replaced by a stochastic function of time [see e..g. [17], eq. (2.2)]. Alternatively, in a non-parametric setup, the transmission function $\pi(.)$ itself can be assumed stochastic. This approach is developed in [23] to account for the varying individual heterogeneity during the outbreak. In a SIR model, this approach accommodates the mover-stayer phenomenon, i.e. the fact that the population at risk is "on average" becoming less vulnerable as time goes on.

This Section discusses the (pseudo) state space representation of structural extensions of type iii), under the presence of both measurement and structural errors.

5.1 The modelling

The simple epidemiological models can be easily extended to allow for time dependent parameters, obtained by replacing θ by $a(t), b$, say, to distinguish the time dependent parameter vector from the constant parameters. Then, their transition model representation

[7] The early literature sometimes assumed that the continuous time measurement errors are independent Gaussian [see [12], p. 148, eq. (A.2)]. Under that assumption there is a discontinuity of the noise process at any time t and the associated stochastic differential equations have no relevant probabilistic meaning. This explains the need for adding instead Brownian motions to the differential system.

involves the transition matrix $\Pi[p(t-1), a(t), b]$. The time dependent propagation parameters can, for instance, capture the time varying implementation of social distancing measures and the compliance with these measures [see e.g. [16], [4]]. Such an extended model can be written also in the (pseudo) state space representation and estimated by using the methods given in the previous Section. The (pseudo) state space representations depend on the assumptions on the evolution of parameter vector $a(t)$. At least three types of modelling approaches can be considered.

i) **Dynamics of $a(t)$ left unspecified**

The (pseudo) state space representation comprises the measurement equation:

$$f(t) = p(t) + u(t),$$

and the transition equations:

$$p(t) = \Pi[p(t-1), a(t), b]' p(t-1).$$

The state variables are the marginal probabilities $p(t)$ and parameters $a(t)$, while b is the vector of constant parameter. They can be jointly estimated and the state variables filtered by the extended Kalman filter, under an identification condition. In particular, the order condition: $(J-1)(T-1) \geq T\, dim\, a + dim\, b$ has to be satisfied.

ii) **Stochastic evolution of $a(t)$**

An alternative model has the same measurement equation and extends the previous (pseudo) state space representation system as it includes additional transitions such as:

$$a^*(t) = \phi a^*(t-1) + v(t),$$

where the errors $v(t)$ are Gaussian noises independent of the measurement errors $u(t)$, a^* is a nonlinear transformation of a, such as $a^* = \log a$ that ensures the positive sign, and $|\phi| < 1$ for stationarity.

Under this representation, the state variables are the marginal probabilities $p(t)$ and parameters $a^*(t)$, and b is the constant parameter vector. The extended Kalman Filter can be used to jointly estimate b and filter the components of $a^*(t)$.

iii) **Exogenous information on $a(t)$**

If the indicators $x(t)$ of social distancing are available, such as counts of travellers [see, [30]], or the daily numbers of fines for disobeying the social distancing rules, the model can be extended to include $x(t)$. Then, the model is similar to the representation above with the autoregressive dynamic replaced by an equation such as:

$$a^*(t) = Cx(t) + v(t)$$

where C is a row vector of constant coefficients to be estimated and $v(t)$ are Gaussian noises independent of the measurement errors $u(t)$.

5.2 Logistic model with stochastic contagion parameter

Let us now examine the limiting case of time independent stochastic contagion parameters, which is a very special case of stochastic dynamics and consider the logistic model of Proposition 2. The stochastic parameters are introduced to account for heterogeneity of infection patterns. For ease of exposition, we assume a discrete heterogeneity distribution with weights $q_k, k = 1, ..., K$ on values $(\alpha_k, \beta_k),\ k = 1, ..., K$ [see, [24], [56]]. Then, equation 3.4 is written conditional on α, β and defines the evolution of $p_{2,k}(t)$ for values α_k, β_k. Next, these evolutions need to be re-integrated with respect to α, β, in order to find the marginal probability of being infected $p_2(t)$ as follows:

$$p_2(t) = \sum_{k=1}^{K} q_k p_{2,k}(t) = \sum_{k=1}^{K} \{q_k [\alpha_k [\exp(\alpha_k + \beta_k)t] - \alpha_k] \,/\, [\alpha_k \exp[(\alpha_k + \beta_k)t] + \beta_k]\}.$$

We get a convex combination of logistic functions [8]. This additive specification implies that $p_2(t)$ cannot follow a quadratic differential equation such as 3.4. There is a double heterogeneity i) in coefficients α, which means that there exist multiple initial exogenous clusters of infection of different sizes, ii) in coefficients β, which means that the speeds of transmission of each cluster are different. This model is not a special case of $(\text{SI})^K$ [see Appendix 1] as there is no contagion between the sub-populations k and only contagion within is allowed.

The presence of heterogeneity in a logistic model generates the following effects:

i) several peaks can appear in the changes in $p_2(t)$ over time. This is the wave effect [see, [53], [24]], due to different transmission parameters of each wave.

[8] used as a basis of functions in neural networks.

ii) the persistence of $p_2(t)$ increases due to the additive representation. This is a well-known long memory effect revealed in [25] for linear autoregressive models that also exists in nonlinear logistic models [see [46]].

Below, a three-wave pattern is illustrated in Figure 9 for the following parameter values: $\alpha = 0.015, 0.0005, 0.0001$, $\beta = 0.95, 0.85, 0.75$

[Insert Figure 9: Three-Wave Infection Pattern]

We observe the three waves with the highest peak due to the first wave. We also observe a persistence effect as the decline following the first peak is slower than the declines of each wave separately.

6 Concluding Remarks

Contrary to the major part of literature on epidemiological models, which considers deterministic continuous time models of counts of individuals in various compartments (states), we consider stochastic models in discrete time for variables representing individual histories [see also [3], [15] for discrete time approach]. The proposed discrete time transition model has the following advantages:

i) It eliminates the lack of consistency between time discretized continuous time models with respect to the time unit. In the continuous time setup, it also eliminates the assumption of differentiability of aggregate counts, which are discrete variables. This is especially important in the early phase of an epidemic when some of these counts are low, but not too low.

ii) The stochastic model allows us to combine different aggregate count variables and individual medical histories of patients under medical care.

iii) The stochastic component allows us for deriving not only the point, but also the interval forecast. This is important at the beginning of an epidemic when the number of observations is small and the results are less reliable.

iv) The estimation of the transition model can be performed by applying an extended Kalman filter to its (pseudo) state space representation.

Appendix A.1

Structural Epidemiological Models

This Appendix presents a typology of basic epidemiological models that can serve as building blocks of more complex specifications. The difference between the basic models are with respect to:

i) the number of states (compartments) and their interpretations as S= susceptible, E=exposed, I =infected, R =recovered, D=deceased.

ii) The number and types of virus propagation sources,

iii) The location of zeros in the transition matrix (i.e. the causal structure),

iv) The structure of time dependent transition probabilities.

We provide below the transition probabilities along with the state interpretations. The time dependent transition probabilities are denoted by π and are functions of (lagged) marginal probabilities $p(t)$.

The models described below are the following:

2-state: SI model, SIS model,

3-state: SIR model,

4-state : SIRD model, SEIR model, SIR model, $(SI)^2$ model, S,IU ,ID, R model.

The interpretations of states and the form of transition matrices are given below. The transmission functions are of a general form in this representation, although in practice, they are often assumed to be linear.

2-state SI model

S= susceptible,I= infected,being immunized and staying infectious for the S people

row 1,S: $\pi_{11}(p_2), \pi_{12}(p_2)$

row 2, I : 0,1

One absorbing state,one source of infection, no collective immunity.

2-state SIS model

S:susceptible, I infected, can recover, but without being immunized.

row 1,S: $\pi_{11}(p_2)$, $\pi_{12}(p_2)$

row 2,I: p_{21}, p_{22}, with $p_{21} > 0$.

One source of infection, no absorbing state; a non degenerate stationary solution can exist, no collective immunity [see e.g. [3], [19], [45] for the use of SIS model].

3-state SIR model
S=susceptible, I= infected, infectious, not immunized, R=recovered, no longer infectious,immunized.
row1,S: $\pi_{11}(p), \pi_{12}(p), 0$
row 2, I: 0, p_{22}, p_{23}
row 3, R: 0,0,1
One absorbing state, one source of infection, collective immunity if the transmission function is linear [see e.g. [48], [41], [31], [27], [49], [23]]. In the basic SIR model, the transmission functions π_{11}, π_{12} depend on p_2 only. They depend on both p_1 and p_2 in extensions accounting for the crowding effects and/or frailty phenomena.

4-state SIRD model
S=susceptible, I=infected, not immunized,infectious, R=recovered, no longer infectious, immunized, D=deceased.

row 1, S: $\pi_{11}(p), \pi_{12}(p), 0, p_{14}$
row 2, I : 0, p_{22}, p_{23}, p_{24}
row 3, R: 0,0, p_{33}, p_{34}
row 4, D: 0,0,0,1
One absorbing state, one propagation source.

4-state $(SI)^2$
The population is divided into 2 sub-populations, as region 1 & region 2, male & female, young & old. It is easily extended to any number of regions, or categories [2].

S_j =susceptible of type j, I_j= infected, immunized, infectious of type j.
row 1, S_1: $\pi_{11}(p_3, p_4), 0, \pi_{13}(p_3, p_4), 0$
row 2, S_2: 0, $\pi_{22}(p_3, p_4), 0, \pi_{24}(p_3, p_4)$
row 3, I_1: 0,0,1,0
row 4,I_2: 0,0,0,1
Two absorbing states,two propagation sources, no collective immunity [see e.g. [19]].

4-state SEIR

S=susceptible E= exposed, but not yet infectious (there is a latency period), not immunized, I = infected and infectious, not immunized, R=recovered,no longer infectious,immunized.

row 1,S: $\pi_{11}(p_3), \pi_{12}(p_3), 0, 0$
row 2,E: 0, $p_{22}, p_{23}, 0$
row 3,I: 0, 0, p_{33}, p_{34}
row 4,R: 0,0,0,1
One absorbing state, one transmission source [see e.g. [57] , [13]].

4-state: S IU ID R
S=susceptible
IU:infected,infectious, not immunized,undetected,
ID: infected,infectious, not immunized,detected,
R:recovered,no longer infectious, immunized.

row 1, S : $\pi_{11}(p_2, p_3), \pi_{12}(p_2, p_3), \pi_{13}(p_2, p_3), p_{14}$
row 2, IU: 0, p_{22}, p_{23}, p_{24}
row 3, ID: 0, 0, p_{33}, p_{34}
row 4, R: 0, 0, 0, 1
One absorbing state, two propagation sources [see e.g. [22]].

These structural models can be extended by considering other states, such as the birth [9] to offset the future number of deaths due to the coronavirus, the types of medical treatment of patients in hospitals, the severity [asymptomatic (mild), symptomatic (high)], or the type of detection (contact tracing, influenza like illness surveillance, tests, etc) [see, e.g. [18]]. The models can also be extended by combining the basic models as building block into 5-state models such as the SEIRD [see e.g. [35]], or S IU ID R D, and 6-state models such as the SIU^2, ID^2 , R, or $(SIR)^2$. The structure of the transition matrix can also be modified to account for the possibility that a fraction of recovered individuals is not entirely immunized and can be infected twice. This leads to a 4-state SIRS model [55].

[9] In transition models the state birth is usually introduced to balance the deaths and to provide stationary evolutions of the processes [see e.g. [27]]. This ad-hoc introduction of births is not relevant when the interest is in determining the nonstationary dynamic at the beginning of the epidemic, rather than in the long run equilibrium. Indeed, the count of births (anticipated 9 months earlier) does not increase in order to offset the increasing number of deaths due to the coronavirus.

Appendix A.2

Rational Recursive Equations

This Appendix shows the exact solution and the exact time discretization of the probability to be infected in a continuous time SI model. We provide below the results for a general one-dimensional Riccati equation in continuous time written on a series $x(t)$. Then, the results can be applied to the special case $x(t) = p_2(t)$.

Such results can be extended to other types of epidemiological models, such as the SIR. This allows for a comparison of continuous time models and some of their Euler discretizations.

i) **The differential equation**
This differential equation is:

$$dx(t)/dt = -\lambda(x(t) - a)(x(t) - b)/(a - b),$$

where λ is strictly positive.

ii) **The exact solution**
Since:

$$(a - b)/[(x(t) - a)(x(t) - b)] = 1/(x(t) - a) - 1/(x(t) - b),$$

we deduce:

$$dx(t)[1/(x(t) - a) - 1/(x(t) - b)] = -\lambda dt,$$

and by integration:

$$|x(t) - a|/|x(t) - b| = exp(-\lambda t)|x(0) - a|/|x(0) - b|.$$

This relation implies that the trajectory $x(t)$ and the starting value $x(0)$ satisfy always the same relationship with respect to a and b, that is $x(t)$ is in the interval (a,b) (resp. below, above), if $x(0)$ is in this interval (resp. below, above). Therefore, we can disregard the absolute values to get:

$$(x(t) - a)/(x(t) - b) = exp(-\lambda t)(x(0) - a)/(x(0) - b),$$

for any nonnegative t.

This implies a logistic expression for $x(t)$:

$$x(t) = [a - bkexp(-\lambda t)]/[1 - kexp(-\lambda t)],$$

where: $k = (x(0) - a)/(x(0) - b)$.

iii) **The exact time discretized recursive model**

We deduce that the exact time discretized counterpart corresponds to a rational transform of $x(t-1)$. More precisely, we get:

$$x(t) = \{a[x(t-1) - b] - b[x(t-1) - a]exp(-\lambda)\}/\{[x(t-1) - b] - [x(t-1) - a]exp(-\lambda)\}.$$

This rational recursive equation, which is the exact time discretization of the differential equations, differs from the crude Euler discretization of the differential equation:

$$x(t) = x(t-1) - \lambda[x(t-1) - a][x(t-1) - b]/(a - b)$$

iv) **Special case**

The results above can be computed for equation 3.4 with: $\lambda = \beta > 0$, $a = -\alpha/\beta, b = 1$. Without an exogenous source of infection: $\alpha = 0$,the interval (a, b) is the interval (0,1), $x(t) = p_2(t)$ is decreasing and tends to 0 when t tends to infinity, for any starting value $p_2(0)$. Therefore, there is no collective immunity, even without an exogeneous source of infection.

vi) **Extensions to SIR model**

Exact solutions of other continuous time epidemiological models have been recently derived from the SIR model with linear and non-linear transmission functions [see, [27], [52], [7], [23]]. These can be used to construct numerical approximations of the continuous trajectories with properties similar to the continuous trajectories themselves.

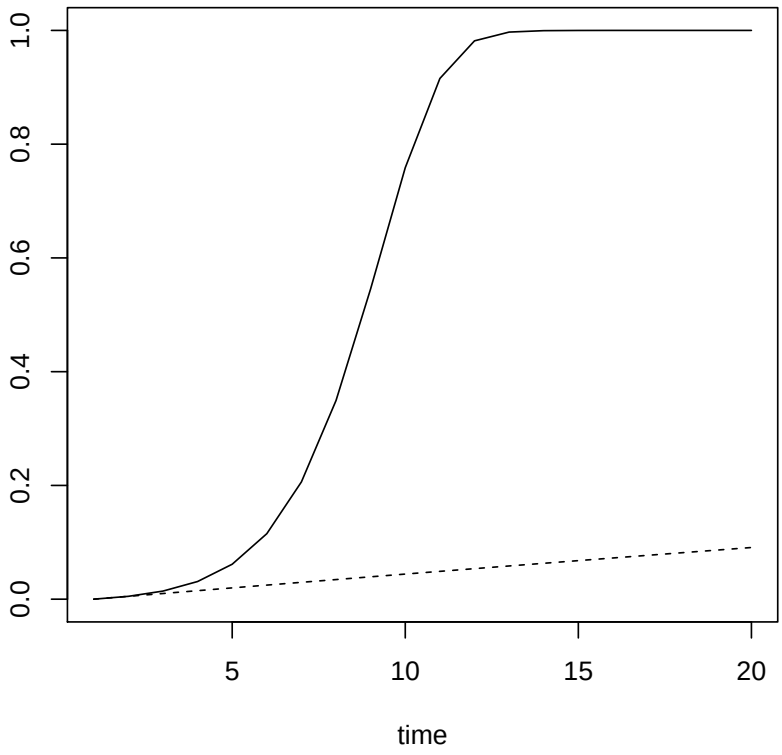

Figure 1: Evolution of $p(t)$, SI Model
Figure 1 shows infection rate $p(t)$ (vertical axis) over 20 days (horizontal axis). Solid line: infection rate of continuous time model (3.4). Dashed line: infection rate of discrete time approximation (3.2)

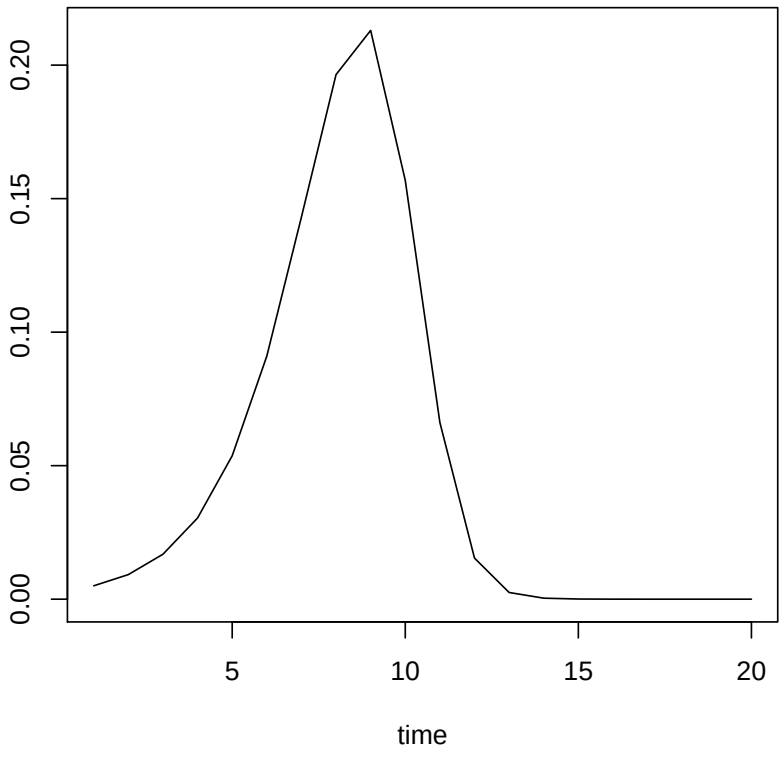

Figure 2: Evolution of Changes in $p(t)$, SI Model
Figure 2 shows changes of infection rate $\Delta p(t)$ (vertical axis) over 20 days (horizontal axis).

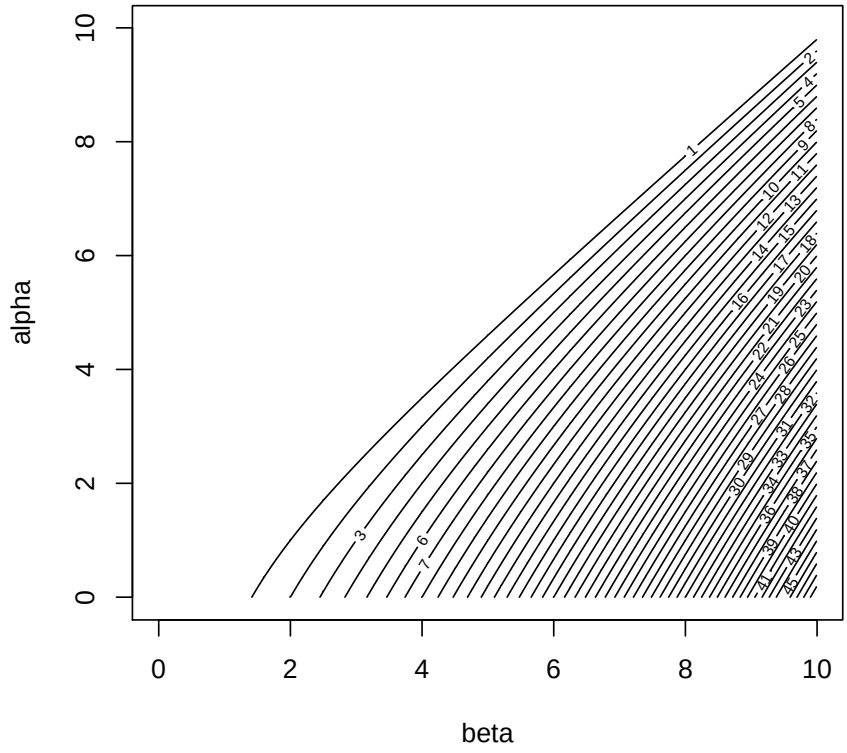

Figure 3: Size of Peak, SI Model
Figure 3 is a contour plot showing the size of peak in $p(t)$ curve, as a function of parameters α and β.

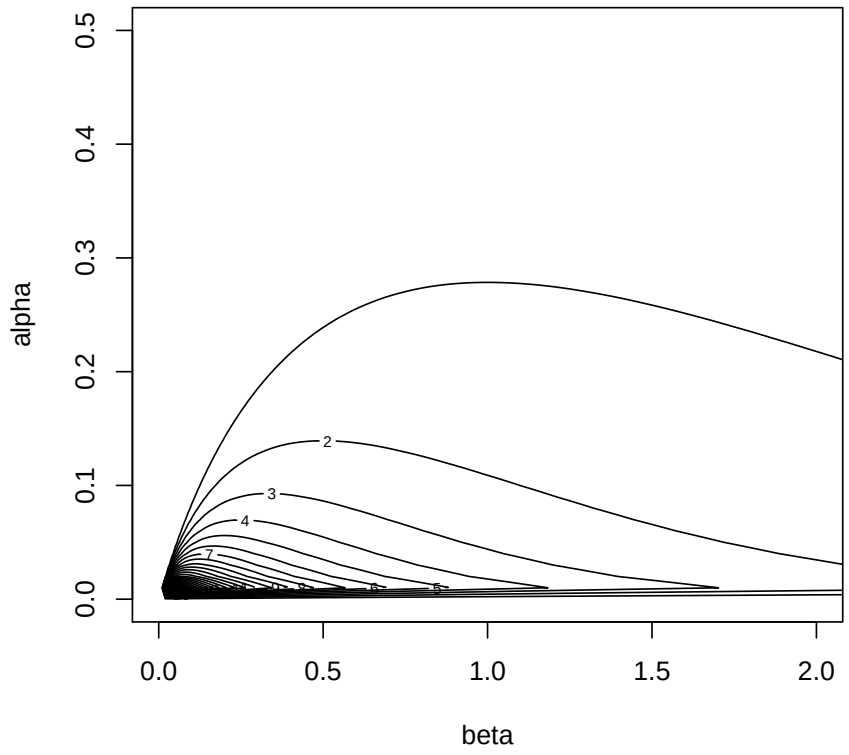

Figure 4: Time to Inflection, SI Model
Figure 4 is a contour plot showing the timing of inflection point in $p(t)$ curve, as a function of parameters α and β.

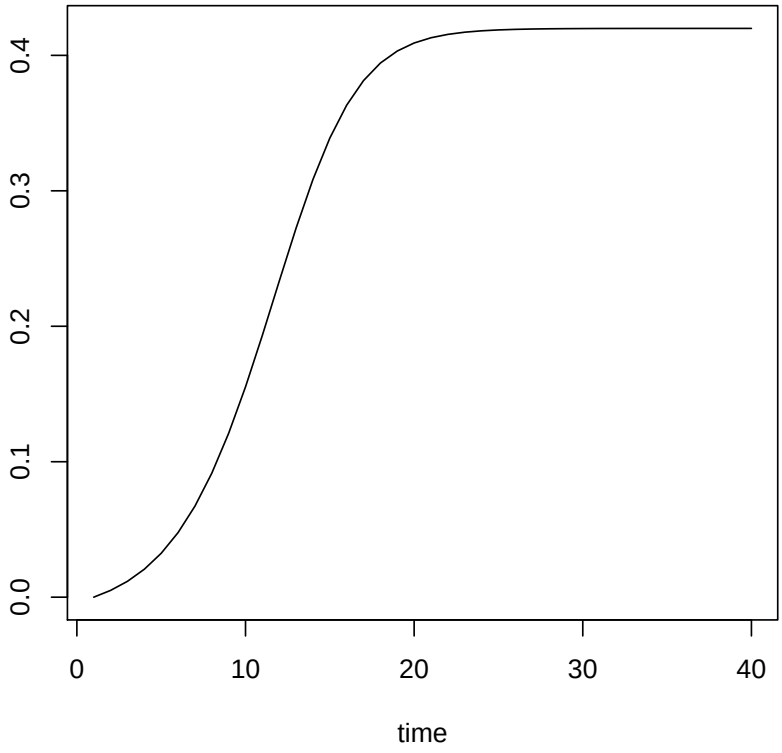

Figure 5: Evolution of $p_2(t)$, SIR Model
Figure 5 shows infection rate $p_2(t)$ (vertical axis) over 40 days (horizontal axis).

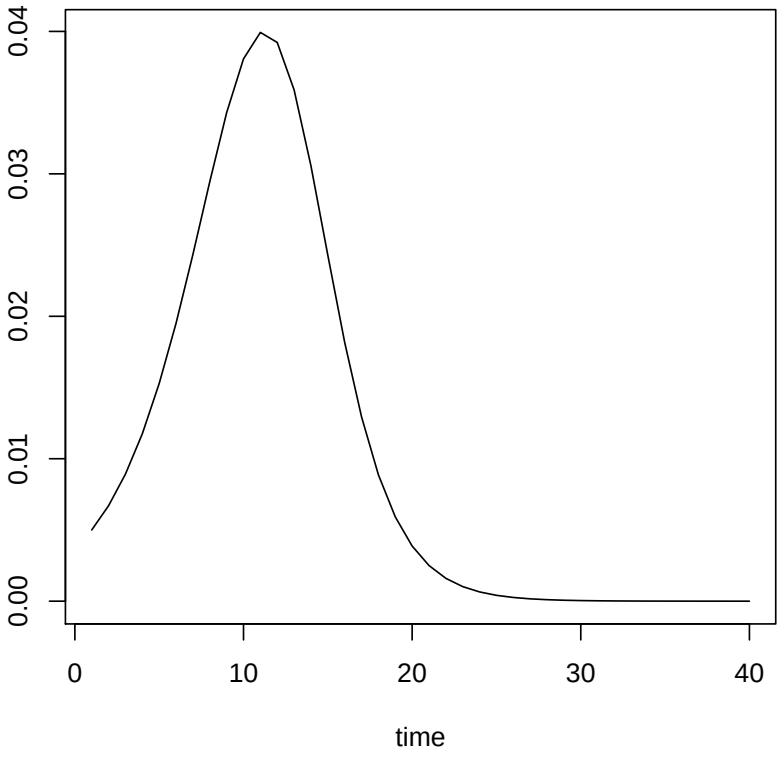

Figure 6: Evolutions of Changes in $p_2(t)$, SIR Model
Figure 6 shows changes of infection rate $\Delta p_2(t)$ (vertical axis) over 40 days (horizontal axis).

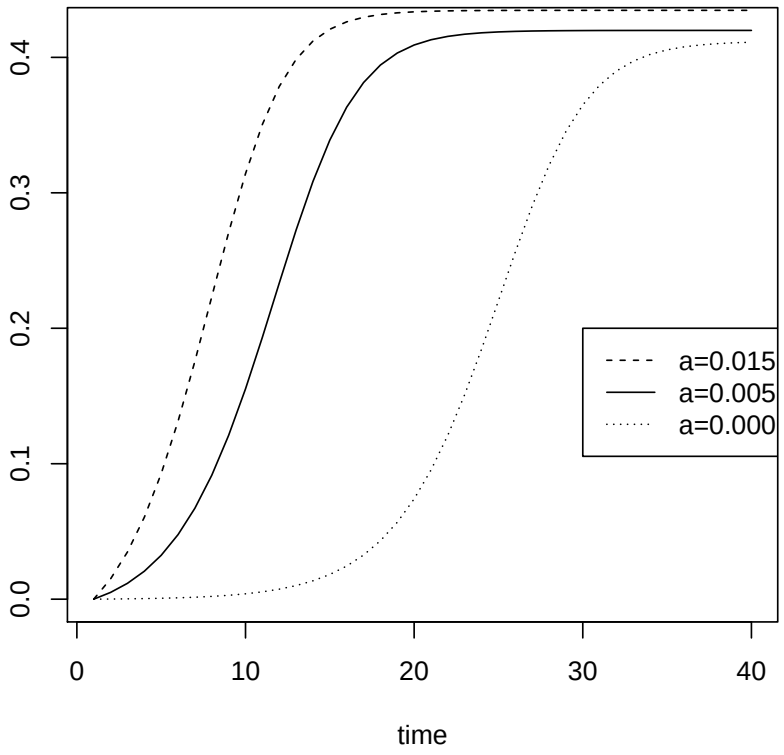

Figure 7: Timing of Peak, a varying, SIR Model
Figure 7 shows infection rates $p_2(t)$ (vertical axis) computed for different values of parameter a over 40 days (horizontal axis)

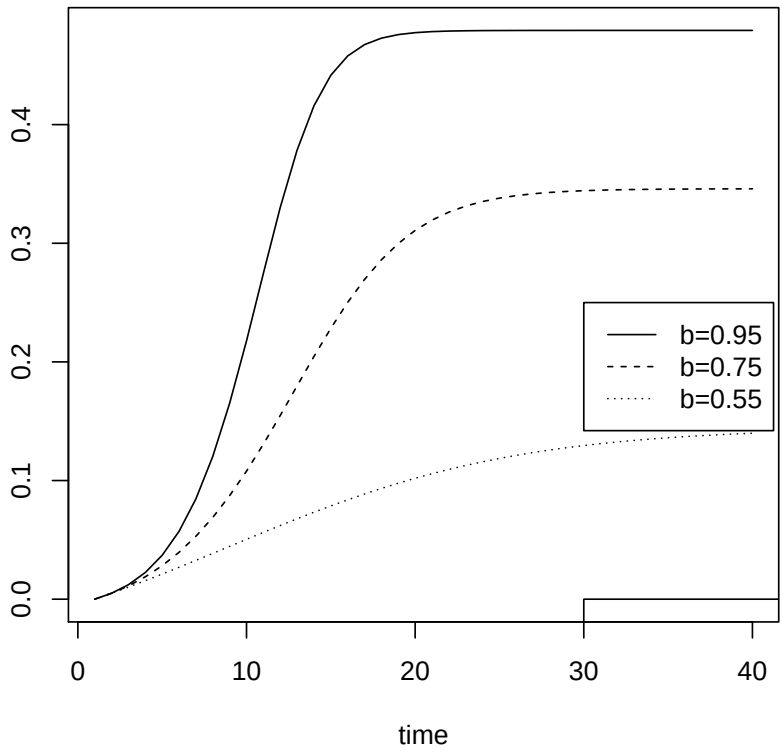

Figure 8: Size of Peak, b varying, SIR Model
Figure 8 shows infection rates $p_2(t)$ (vertical axis) computed for different values of parameter b over 40 days (horizontal axis)

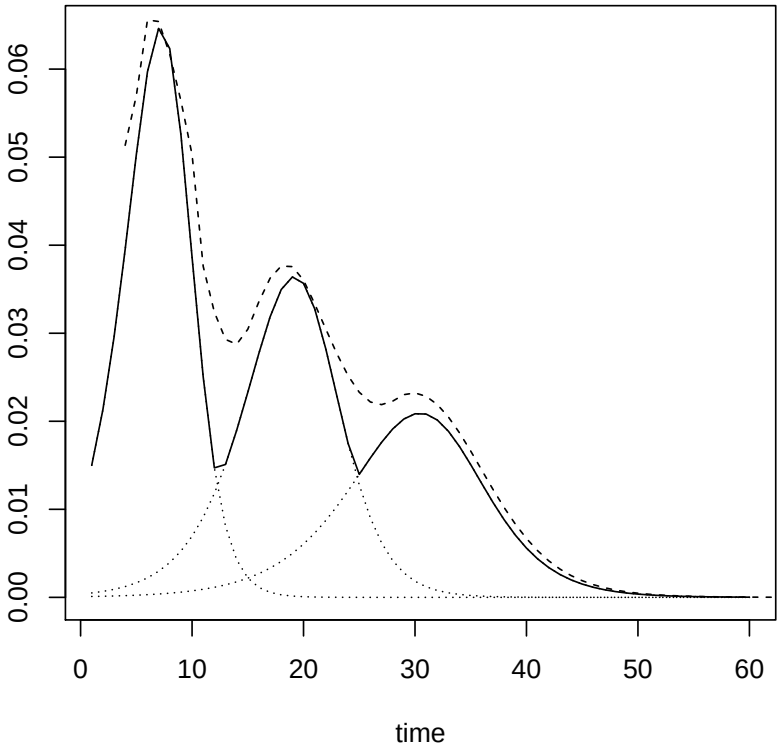

Figure 9: Three-Wave Infection Pattern
Figure 9 shows infection rate $p_2(t)$ (vertical axis) with time varying parameters a and b, over 40 days (horizontal axis)

References

[1] J Admani, K Hattaf, and N Yousfi. Dynamical Behaviour of a Stochastic SIRS Epidemic Model. *Journal of Mathematical and Computational Science*, 8:421–431, 2018.

[2] A Alipoor and O Boldea. The Role of the Elementary Schools in SARS-Cov 2 Transmission. Working Paper Tilburg University, 2020.

[3] L Allen. Some Discrete-Time SI, SIR and SIS Epidemic Models. *Mathematical Biosciences*, 124:83–105, 1994.

[4] F Alvarez, D Argente, and F Lippi. A Simple Planning Problem for COVID-19 Lockdown. DP LUISS and Einaudi Institute for Economics and Finance, 2020.

[5] D Anderson and R Watson. On the Spread of Disease with Gamma Distributed Latent and Infectious Periods. *Biometrika*, 67:191–198, 1980.

[6] J Berkson. Application of the Logistic Function to Bio-Assay. *JASA*, pages 339–357, 1944.

[7] M Bohner, S Streipert, and D Torres. Exact Solution of a Dynamic SIR Model. *Nonlinear Analysis: Hybrid System*, 32:228–238, 2019.

[8] H Brandenburg. Piecewise Quadratic Growth During the 2019 Novel Coronavirus Epidemic. *Infectious Disease Modelling*, 5:681–690, 2020.

[9] F Brauer and C Castillo-Chavez. *Mathematical Models in Population Biology and Epidemiology*. Springer, 2001.

[10] C Breto, D He, E Ionides, and A King. Time Series Analysis via Mechanistic Models. *Annals of Applied Statistics*, 3:319–348, 2009.

[11] G Brown, E Ghysels, and L Yi. Estimating Undetected COVID-19 Infections: The Case of North Carolina. DP University of North Carolina, 2020.

[12] B Cazelles and N Chau. Using the Kalman Filter and Dynamic Models to Assess the Changing HIV/AIDS Epidemic. *Mathematical Biosciences*, 140(131-154), 1997.

[13] D Champredon, J Dushoff, and D Earn. Equivalence of the Erlang-Distributed SEIR Epidemic Model and the Renewal Equation. *SIAM Journal of Applied Mathematics*, 78:3258–3270, 2018.

[14] G Chowell, A Tariq, and J M Hyman. A Novel Sub-Epidemic Modeling Framework for Short Term Forecasting Epidemic Waves. *BMC Med*, 17:1–19, 2019.

[15] P Das, D Mukherjee, and A Sarkar. Study of an SI Epidemic Model with Non-linear Incidence Rate: Discrete and Stochastic Version. *Applied Mathematics and Computation*, 218:2509–2515, 2011.

[16] L DiDomenico, G Pullano, P Coletti, N Hens, and V Colizza. Expected Impact of School Closure and Telework to Mitigate COVID-19 Epidemic in France. www.epicx-lab.com/covid-19.html, 2020.

[17] J Dureau, K Kalogeropoulos, and M Baguelin. Capturing the Time Varying Drivers of an Epidemic Using Stochastic Dynamical Systems. *Biostatistics*, 14:541–555, 2013.

[18] Verity et al. Generalized Estimates of the Severity of Coronavirus Disease 2019: A Model Based Analysis. available online, 2020.

[19] Z Feng, W Huang, and C Castillo-Chavez. Global Behaviour of a Multi Group SIS Epidemic Model with Age Structure. *Journal of Differential Equations*, 218:292–314, 2005.

[20] V Godambe and M Thompson. Estimating Equations in the Presence of a Nuisance Parameter. *Annals of Statistics*, 3:568–576, 1974.

[21] C Gourieroux and J Jasiak. Multivariate Jacobi Process with Smoothed Transition. *Journal of Econometrics*, 131:475–505, 2006.

[22] C Gourieroux and J Jasiak. Time Varying Markov Processes with Partially Observed Aggregate Data: An Application to Coronavirus. *Journal of Econometrics*, 2020. forthcoming.

[23] C Gourieroux and Y Lu. SIR Model with Stochastic Transmission. DP CREST, 2020.

[24] C Gourieroux and I Peaucelle. Diffusion and Wave Effects. *Annales d'Economie et de Statistique*, 44:191–217, 1996.

[25] C Granger and A Joyeux. An Introduction to Long Memory Time Series Models and Fractional Differencing. *Journal of Time Series Analysis*, 1:15–29, 1980.

[26] J Hardin and J Hilbe. *Generalized Estimating Equations*. Chapman Hall, 2003.

[27] T Harko, F Lobo, and M Mak. Exact Analytical Solutions of the Susceptible-Infected-Recovered Epidemic Model and of the SIR Model with Equal Death and Birth Rates. *Applied Mathematics and Computation*, 236:184–194, 2014.

[28] A Harvey and P Kattuman. Time Series Models Based on Growth Curves with Applications to Forecasting Coronavirus. *Covid Economics*, 24:126–157, 2020.

[29] H Hethcote. The Mathematics of Infectious Diseases. *SIAM Review*, 42:599–653, 2000.

[30] A Hortescu, J Liu, and T Schwieg. Estimating the Fraction of Unreported Infections in Epidemics with a Known Epicenter: An Application to COVID-19. DP University of Chicago, 2020.

[31] D Jiang, J Yu, C Ji, and N Shi. Asymptotic Behaviour of Global Positive Solution to a Stochastic SIR Model. *Mathematical and Computer Modelling*, 54:221–232, 2011.

[32] J Kalbfleisch, J Lawless, and W Vollmer. Estimation in Markov Models from Aggregate Data. *Biometrics*, 39:907–919, 1983.

[33] W Kermack and A McKendrick. A Contribution to the Mathematical Theory of Epidemics. *Proceedings of the Royal Statistical Society A*, 115:700–721, 1927.

[34] A King, M de Celles, F Magpantay, and P Rohani. Avoidable Errors in the Modelling of Outbreaks of Emerging Pathogens with Special Reference to Ebola. *Proceeding of the Royal Statistical Society B Biological Science*, 282, 2015.

[35] I Korolev. Estimating the Parameters of the SEIRD Model for COVID-19 Using the Deaths Data. DP Binghamton University, 2020.

[36] A El Koufi, J Adnani, A Bennar, and N Yousfi. Analysis of a Stochastic SIR Model with Vaccination and Nonlinear Incidence Rate. *International Journal of Differential Equations*, 2019(ID 9275051), 2019.

[37] A Krener. *The Convergence of the EKF, Directions in Mathematical Systems: Theory and Optimization*. Springer, 2003.

[38] O Krylova and D Earn. Effects of the Infectious Period Distribution on Predicted Transitions in Childhood Disease Dynamics. *J. Royal Soc., Interface*, 10(20130098), 2013.

[39] D Kuhi, E Kebraeb, S Lopez, and J France. An Evaluation of Different Growth Functions for Describing the Profile of Live Weight with Age in Meat and Egg Strains of Chicken. *Poultry Science*, 82:1536–1543, 2003.

[40] E McRae. Estimation of Time Varying Markov Processes with Aggregate Data. *Econometrica*, 45:183–198, 1977.

[41] X Meng and L Chen. The Dynamics of a New SIR Epidemic Model Concerning Pulse Vaccination Strategy. *Applied Mathematics and Computation*, 197:582–597, 2008.

[42] J Miller and G Judge. Information Recovery in a Dynamic Statistical Markov Model. *Econometrics*, 3/2:187–198, 2015.

[43] N Nihan and G Davis. Recursive Estimation of Origin-Destination Matrices From Input/Output Counts. *Transpn. Research*, 218:149–163, 1987.

[44] F Richards. A Flexible Growth Function for Empirical Use. *J. Exp. Bot.*, 10:290–301, 1959.

[45] R Rifhat, L Wang, and Z Teng. Dynamics for a Class of Stochastic SIS Epidemic Models with Nonlinear Incidence and Periodic Coefficients. *Physica A*, 48:176–190, 2017.

[46] L Sattenspeil. Modeling the Spread and Persistence of Infectious Disease in Human Populations. Yearbook of Physical Antropology, 1990.

[47] Y Song and J Grizzle. The Extended Kalman Filter as a Local Asymptotic Observer. *Estimation and Control*, 5:59–78, 1995.

[48] J Tchuenche, A Nwagwo, and R Levins. Global Behaviour of an SIR Epidemic Model with Time Delay. *Mathematical Methods in Applied Sciences*, 30:733–749, 2007.

[49] A Toda. Susceptible-Infected-Recovered (SIR): Dynamics of COVID-19 and Economic Impact. ArXiv:2003.11221v2, 2020.

[50] C Viboud, L Simonsen, and G Chowell. A Generalized Growth Model to Characterize the Early Ascending Phase of Infectious Disease Outbreaks. *Epidemics*, 15:27–37, 2016.

[51] E Vynnicky and R White, editors. *An Introduction to Infectious Disease Modelling*. Oxford Univ. Press, 2010.

[52] H Williams, I Mazilu, and D Mazilu. Stochastic Epidemic-Type Model with Enhanced Connectivity: Exact Solution. *Journal of Statistical Mechanics: Theory and Experiment*, 1, 2018.

[53] G Witham. *Linear and Nonlinear Waves*. Wiley, 1974.

[54] K Wu, D Darcet, Q Wang, and D Sornette. Generalized Logistic Growth Modelling of the COVID-19 Outbreak in 29 Provinces in China and in the Rest of the World. DP ETH Zurich, 2020.

[55] C Xu and X Li. The Threshold of a Stochastic Delayed SIRS Epidemic Model with Temporary Immunity and Vaccination. *Solitons and Fractals*, 111:227–234, 2018.

[56] P Yan and G Chowell. *Quantitative Methods for Investigating Infectious Disease Outbreaks*. Springer, 2019.

[57] I Zhang and Z Ma. Global Dynamics of a SEIR Epidemic Model with Saturating Contact Rate. *Mathematical Biosciences*, 185:15–32, 2003.